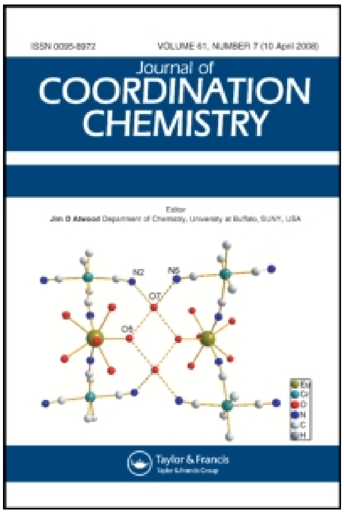

Journal of Coordination Chemistry
Publication details, including instructions for authors and subscription information:
http://www.informaworld.com/smpp/title~content=t713455674

Ni(II) complexes of unsymmetrical phenyl and phenethyl dithiocarbamates and triphenylphosphine

Richard Pastorek[a]; Jiří Kameníček[a]; Helena Vrbová[a]; Václav Slovák[b]; Marek Pavlíček[a]
[a] Department of Inorganic Chemistry, Palacký University, 77147 Olomouc, Czech Republic [b] Faculty of Science, Department of Chemistry, University of Ostrava, 70103 Ostrava, Czech Republic

To cite this Article Pastorek, Richard , Kameníček, Jiří , Vrbová, Helena , Slovák, Václav and Pavlíček, Marek(2006) 'Ni(II) complexes of unsymmetrical phenyl and phenethyl dithiocarbamates and triphenylphosphine', Journal of Coordination Chemistry, 59: 4, 437 — 444

To link to this Article: DOI: 10.1080/00958970500490798

URL: http://dx.doi.org/10.1080/00958970500490798

Journal of Coordination Chemistry
Vol. 59, No. 4, March 2006, 437–444

Taylor & Francis
Taylor & Francis Group

Ni(II) complexes of unsymmetrical phenyl and phenethyl dithiocarbamates and triphenylphosphine

RICHARD PASTOREK†, JIŘÍ KAMENÍČEK*†, HELENA VRBOVÁ†,
VÁCLAV SLOVÁK‡ and MAREK PAVLÍČEK†

†Department of Inorganic Chemistry, Palacký University,
Křížkovského 10, 77147 Olomouc, Czech Republic
‡Faculty of Science, Department of Chemistry, University of Ostrava,
30 dubna 22, 70103 Ostrava, Czech Republic

(*Received in final form 10 October 2005*)

Unsymmetrical Ni(II) complexes of phenyl- and phenethyldithiocarbamate and PPh_3 of composition $[NiX(HPhdtc)(PPh_3)]$, $[NiX(HPhetdtc)(PPh_3)]$, $[Ni(HPhdtc)(PPh_3)_2]ClO_4$ and $[Ni(HPhdtc)(PPh_3)_2]PF_6$ {X = Cl, Br, I, NCS; HPhdtc = phenyldithiocarbamate, HPhetdtc = phenethyldithiocarbamate, PPh_3 = triphenylphosphine} have been synthesized. The complexes have been characterized by elemental and thermal analysis, IR and electronic spectroscopy, magnetochemical and conductivity measurements. Single-crystal X-ray analysis of $[NiBr(HPhdtc)(PPh_3)] \cdot CHCl_3$ confirmed a distorted square planar coordination for the NiS_2PBr chromophore. For selected samples, the catalytic effects of graphite oxidation were studied.

Keywords: Nickel(II)-dithiocarbamate; Triphenylphosphine; X-ray structure; Graphite oxidation

1. Introduction

Some unsymmetrical Ni(II) dithiocarbamates with PPh_3 ligands have recently been described [1–5]. These are compounds with the NiS_2PX chromophore of composition $[Ni(NO)(HRdtc)(PPh_3)]$ (R = methyl, ethyl, butyl, phenyl, *p*-chlorphenyl, *p*-methoxyphenyl, dtc = S_2CN); $[NiX(HRdtc)(PPh_3)]$ (X = Cl, Br, I, NCS, R = methyl, ethyl, butyl, phenyl, *p*-chlorphenyl, *p*-methoxyphenyl, 2-hydroxyethyl, 2,3-dimethyl-1-phenyl-3-pyrazolin-5-on-4-yl). Complexes with the NiS_2P_2 chromophore of the $[Ni(HRdtc)(PPh_3)_2]ClO_4$ {R = methyl, carboxymethyl, 2-(2-indolyl)-1-carboxyethyl} [3, 6] have also been reported, but no X-ray structure is available. For Ni(II) phenyl- and phenethyldithiocarbamates, only $[NiBr(HPhetdtc)(PPh_3)]$ has been reported [2].

In this article, the syntheses of new complexes of composition $[NiX(HRdtc)(PPh_3)]$ and $[Ni(HPhdtc)_2]Y$ are described. Attention is drawn to the influence of donor atoms,

---

*Corresponding author. Email: kamen@prfnw.upol.cz

Journal of Coordination Chemistry
ISSN 0095-8972 print: ISSN 1029-0389 online © 2006 Taylor & Francis
DOI: 10.1080/00958970500490798

R group and Y anion on structure. In some cases, we used thermal analysis to study the catalytic influence of complexes on graphite oxidation. Graphite is frequently used as an ideal carbon model. It is known that results obtained for graphite oxidation in the presence of inorganic compounds can also be used for another coal material (metallurgical coke). An understanding of the oxidative pyrolysis mechanism of these species with inorganic admixtures is important for many industrial applications (metal production, metallurgical waste, especially for coal oxidation).

2. Experimental

2.1. *Materials*

Graphite was supplied by Fluka and phenethylamine and triphenylphosphine by Sigma Aldrich. Remaining reagents were obtained from Lachema, all of p.a. purity.

2.2. *Syntheses*

2.2.1. [NiX(HRdtc)(PPh_3)] (X = Cl, Br, I, NCS; R = Ph, Phet). Solutions of [Ni(HRdtc)$_2$] [7] and [NiX$_2$(PPh_3)$_2$] [8] (1 mmol) in 20 cm^3 of chloroform at room temperature were filtered through active carbon. After addition of diethylether (6 cm^3), crystals of [NiBr(HPhdtc)(PPh_3)] · $CHCl_3$ (**II**) suitable for X-ray analysis were obtained. In the case of Ni(NCS)(HPhdtc)(PPh_3)] (**IV**), the powder obtained was separated by filtration and washed with *n*-hexane; for [NiCl(HPhdtc)(PPh_3)] (**I**) and [NiI(HPhdtc)(PPh_3)] (**III**), evaporation of solvent and addition of *n*-hexane was necessary. [NiCl(HPhetdtc)(PPh_3)], [NiBr(HPhetdtc)(PPh_3)], [NiI(HPhetdtc)(PPh_3)] and [Ni(NCS)(HPhetdtc)(PPh_3)], (**V–VIII**), respectively were obtained from viscous solutions by addition of *n*-hexane. All solids were washed with *n*-hexane and dried at 40°C under an infrared lamp. Yields: 76% (**I**), 80% (**II**), 73% (**III**), 83% (**IV**), 72% (**V**), 77% (**VI**), 88% (**VII**), 77% (**VIII**).

2.2.2. [Ni(HPhdtc)(PPh_3)$_2$]Y (Y = ClO_4, PF_6). A suspension of finely powdered [Ni(HPhdtc)$_2$] (1 mmol), PPh_3 (2 mmol) and $NiCl_2 \cdot 6H_2O$ (1 mmol) in 20 cm^3 of methanol was stirred under reflux for 1 h. Finely powdered $LiClO_4 \cdot 3H_2O$ or K[PF_6] (1 mmol) was then added and the mixture was stirred for a further hour. A small amount of active carbon was added and the solution filtered and slowly evaporated to near dryness. Products were obtained by dissolution of the residue in $CHCl_3$ and precipitation by addition of *n*-hexane. Solids were filtered off, washed with *n*-hexane and dried under an infrared lamp at 40°C. Yields: 77% ([Ni(HPhdtc)(PPh_3)$_2$]ClO_4, **IX**), 72% ([Ni(HPhdtc)(PPh_3)$_2$]PF_6, **X**).

2.3. *Physical measurements*

The nickel content was determined by chelatometric titration using murexid as indicator [9]. Chlorine, bromine and iodine were determined by the Schöniger

Table 1. Crystal data and structure refinement details for $[NiBr(HPhdtc)(PPh_3)]\cdot CHCl_3$.

Empirical formula	$C_{26}H_{22}BrCl_3NNiPS_2$
Formula weight	688.51
Temperature (K)	100(2)
Wavelength (Å)	0.71073
Crystal size (mm^3)	$0.4 \times 0.2 \times 0.2$
Crystal system, space group	Monoclinic, $P2_1/c$
Unit cell dimensions (Å, °)	$a = 13.697(3)$, $b = 22.216(4)$, $c = 9.672(2)$, $\beta = 109.45(3)$
V (Å^3)	2775.2(10)
Z, calculated density ($Mg\,m^{-3}$)	4, 1.648
Absorption coefficient (mm^{-1})	2.654
Extinction coefficient	0.0007(8)
F (000)	1384
θ range for data collection (°)	3.27–32.10
Index ranges	$-20 \le h \le 19$, $-32 \le k \le 32$, $-9 \le l \le 14$
Reflections collected/unique	29738/8864 [R(int) = 0.0932]
Completeness to $2\theta = 32.1°$	89.2%
Refinement method	Full-matrix least-squares on F^2
Data/restraints/parameters	8864/0/317
Goodness-of-fit on F^2	1.099
Final R indices [$I > 2\sigma(I)$]	$R_1 = 0.0906$, $wR_2 = 0.2447$
R indices (all data)	$R_1 = 0.1259$, $wR_2 = 0.2727$
Largest diff. peak and hole (e Å^{-3})	2.339 and −2.181

method [10]. CHNS analyses were performed on a Fisons EA 1108 instrument. Satisfactory analyses for all complexes described above were obtained. Room temperature magnetic susceptibilities were measured by the Faraday method using $Co[Hg(NCS)_4]$ as calibrant on a laboratory-designed instrument based on a Sartorius 4434 MP-8 microbalance. Conductivities were measured with an LF 330 meter (WTW GmbH) at 25°C. Diffuse reflectance electronic spectra (40,000–11,000 cm^{-1}) were measured on a Specord M 40 spectrophotometer and IR spectra (4,000–400 cm^{-1}) were recorded on a Specord M 80 instrument using nujol mulls. Thermal analysis was performed on a Seiko 6200 TG/DTA instrument with a heating rate of 5°C min^{-1}, sample weights of 8.90 to 11.7 mg and a temperature range of 20–1000°C.

Catalytic graphite oxidation was followed on a Netzsch STA 449C device with an α-Al_2O_3 crucible without standard, with a heating rate of 10°C min^{-1}, a sample weight of 5.0 mg and in a dynamic atmosphere (air, 100 $cm^3\,min^{-1}$). Samples were prepared by mixing graphite (0.6 g, diameter of particles less than 0.1 mm, ash residue max. 0.2%, mass drying loss max. 0.2%) and an acetone solution (2 cm^3) of the appropriate complex (**IV**, **V**, **IX**); $[Ni] = 2.5 \cdot 10^{-3}\,mol\,dm^{-3}$ and pure acetone – (sample **0**; see below). All samples were homogenized by stirring and dried at room temperature for 24 h. Kinetic parameters were calculated by a direct non-linear regression method [11].

2.4. *Crystal structure*

X-ray data collection for $[NiBr(HPhdtc)(PPh_3)]\cdot CHCl_3$ (**II**) was performed on an Oxford Diffraction Xcalibur^{TM}2 four-circle κ-axis diffractometer equipped with a Sapphire2 CCD detector and a Cryojet cooler system, using Mo-Kα radiation at 100 K. The CrysAlis program package (V1.171.7, Oxford Diffraction) was used for

Table 2. Selected bond lengths (Å) and angles (°) for $[NiBr(HPhdtc)(PPh_3)]\cdot CHCl_3$.

Ni(1)–P(1)	2.1961(17)	P(1)–Ni(1)–S(2)	96.05(7)
Ni(1)–S(1)	2.2128(16)	P(1)–Ni(1)–Br(1)	94.00(5)
Ni(1)–S(2)	2.1814(16)	S(1)–Ni(1)–S(2)	78.38(6)
Ni(1)–Br(1)	2.3323(10)	S(1)–Ni(1)–Br(1)	92.20(5)
S(1)–C(1)	1.694(6)	N(1)–C(1)–S(1)	129.9(5)
S(2)–C(1)	1.730(7)	N(1)–C(1)–S(2)	121.8(5)
C(1)–N(1)	1.329(8)	C(1)–S(1)–Ni(1)	86.2(2)
N(1)–C(2)	1.436(8)	C(1)–S(2)–Ni(1)	86.4(2)
P(1)–C(11)	1.822(6)	S(1)–C(1)–S(2)	108.3(3)
P(1)–C(21)	1.826(7)	N(1)–C(1)–S(1)	130.1(5)
P(1)–C(31)	1.823(6)	N(1)–C(1)–S(2)	121.6(5)
		C(1)–N(1)–C(2)	125.8(6)

Table 3. Possible hydrogen bonds for $[NiBr(HPhdtc)(PPh_3)]\cdot CHCl_3$.

Donor–H	Donor···Acceptor	H···Acceptor	Donor-H···Acceptor
C3–H3	C3···S1	H3···S1	C3–H3···S1
0.960(0.058)	3.180(0.054)	2.636(0.011)	116.25(0.57)
1.080		2.585	113.87[a]
C36–H36	C36···Br1	H36···Br1	C36–H36···Br1
0.960(0.163)	3.620(0.185)	2.949(0.016)	127.98(1.14)
1.080		2.877	126.09[a]
C3–H3	C3···S2	H3···S2	C3–H3···S2
0.960(0.058)	3.279(0.114)	2.421(0.032)	148.66(0.26)
1.080		2.319	147.12[a]

[a] Values normalized following G.A. Jeffrey and L. Lewis. *Carbohydr. Res.*, **60**, 179 (1978); R. Taylor, O. Kennard. *Acta Cryst.*, **B39**, 133 (1983).

data reduction. The structure was solved by direct methods using SHELXS-97 [12]; XABS22 absorption and extinction corrections were applied. The structure was refined anisotropically for all non-hydrogen atoms by full-matrix least-squares procedures using SHELXL-97 [13]; hydrogen atoms were refined isotropically. Additional calculations were performed using the PARST program [14]. X-ray data are given in tables 1–3.

3. Results and discussion

Characteristic physical data for the complexes are given in table 4. All complexes are diamagnetic. $[NiX(HRdtc)(PPh_3)]$ species are non-electrolytes and $[Ni(HPhdtc)(PPh_3)_2]Y$ species are 1 : 1 electrolytes in nitromethane solution [15]. This is in agreement with the assumption of a square planar arrangement of the coordination spheres. The ionic nature of ClO_4^- and PF_6^- was supported by IR spectra of $[Ni(HPhdtc)(PPh_3)_2]Y$ complexes. For $Y = ClO_4^-$ ν_3 and ν_4 were observed at 1082^{-1} and at $626\,cm^{-1}$, respectively [16]; for $Y = PF_6^-$ a band at $836\,cm^{-1}$ was found [17]. For $[Ni(NCS)(HRdtc)(PPh_3)]$ complexes, coordination of NCS to the nickel via nitrogen atom was indicated. Vibrations ν(C≡N) at 2102 to $2112\,cm^{-1}$ and ν(C–S) at 824 to $832\,cm^{-1}$ were recorded [18]. IR spectra of all complexes exhibit typical ν(C–S) vibrations at 972 to $994\,cm^{-1}$, ν(C–N) vibrations at 1510 to $1524\,cm^{-1}$ and ν(N–H) vibrations at 3100 to $3188\,cm^{-1}$ [2, 19]. Square planar coordination of the nickel is also

Table 4. Characteristic data for the complexes.

			IR [cm^{-1}]							
	Colour	λ_M^a [$S\,cm^2\,mol^{-1}$]	ν(N–H)	ν(C–N)	ν(C–S)		Abs max. $\times 10^3\,cm^{-1}$	B^b	E_n [°C]	E_x
I	Deep brown	2.6	3121w	1521m	988s		20.1; 29.9; 38.9	94	129.2	171.5
II	Deep brown	4.9	3116m	1516m	980m		20.0; 28.1	45.2	122.5	181.9
III	Dark	1.3	3112w	1520m	990m		18.3; 23.0; 30.0	46.3	59.8	150.2
IV	Light red	2.4	3100m	1524m	972s	ν(C≡N): 2102s; ν(C–S): 824s	20.6; 29.2	109.8	107.8	160.4
V	Deep red	2.7	3118m	1516s	992m		19.2; 30.6	117.6	77.9	172.4
VI	Deep brown	3.6	3146w	1520s	994m		19.2; 30.4	113.9	77.0	175.6
VII	Deep brown	5.0	3188w	1520s	994m		18.1; 30.0	50.1	126.6	165.0
VIII	Violet	2.4	3126m	1520s	983s	ν(C≡N): 2112s; ν(C–S): 832s	19.8; 29.0; 35.2	134.9		159.0
IX	Light brown	77	3110m	1520m	980m	$\nu_3(ClO_4^-)$: 1082s; $\nu_4(ClO_4^-)$: 626m	18.0			
X	Yellow	72	3142m	1510w	986s	$\nu(PF_6^-)$: 836m	18.3; 30.1	76.7	104.4	

[a] In nitromethane solution, $[Ni^{2+}] = 10^{-3}\,mol\,dm^{-3}$; [b] B = start of thermal decomposition; E_x = peak of exotherm; E_n = peak of endotherm.

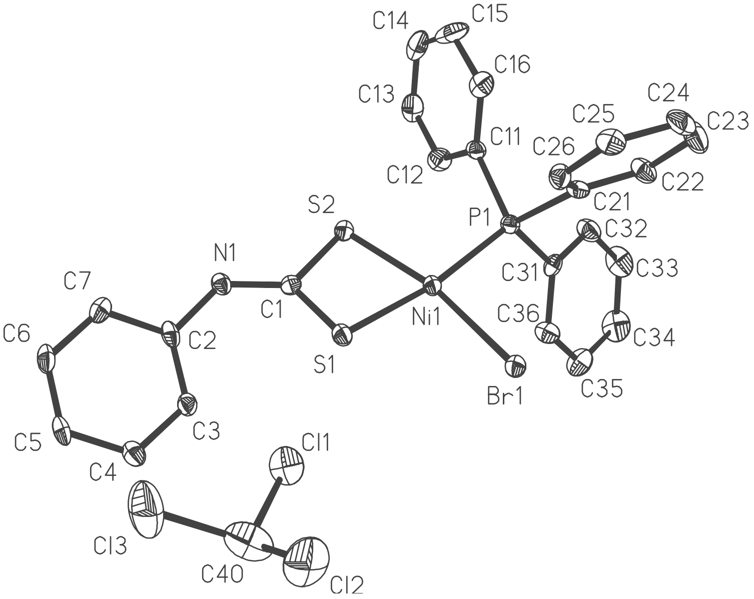

Figure 1. ORTEP drawing of $[NiBr(HPhdtc)(PPh_3)] \cdot CHCl_3$ with the atom labelling scheme. Thermal ellipsoids are drawn at the 40% probability level and hydrogen atoms are omitted for clarity.

supported by reflectance spectroscopy (in nujol); the strong bands in the 18,000 to 23,000 cm^{-1} region can be assigned to d–d transitions typical of square planar nickel(II) [20, 21]. Bands over 30,000 cm^{-1} are probably connected with intraligand transitions of the S_2CN^- group [22].

The X-ray structure of $[NiBr(HPhdtc)(PPh_3)] \cdot CHCl_3$ (figure 1) confirmed these conclusions. This is apparent from the Ni–S, Ni–P and Ni–Br bond lengths and angles in the NiS_2PBr chromophore. Deviations of the chromophore atoms from the ideal NiS_2PBr plane are Ni(1) −0.013(9), S(1) −0.14(2), S(2) 0.17(2), P(1) −0.12(2), Br(1) 0.024(8) Å. A significant π-bond component in C(1)–N(1), C(1)–S(1) and C(1)–S(2) is evident (see table 2); bond lengths are somewhat shorter than values for simple σ(C–N) and σ(C–S) bonds (1.47 and 1.81 Å) [23]. The $CHCl_3$ molecule is positioned out of the coordination sphere with Ni(1)–C(40) = 7.077 Å. Significant disorder of $CHCl_3$ solvate was observed, which led to the high values of residual electron density in the final electron density map situated near the Cl(3) atom. Possible hydrogen bonds in the lattice are listed in table 3.

Thermal decomposition of the complexes starts between 45 and 135°C (see table 4). The processes are complex with no stable intermediates, and were not studied in detail. Clearly apparent were small endotherms for **V** and **VI** at 78 and 77°C, respectively, connected with melting (confirmed by melting point apparatus). Small exotherms for all complexes observed in the range 159–182°C (for **I**, **IV**, **V**, **VI**, and **VIII** with a small mass increase in TG) could be explained by insertion of oxygen into the Ni–P bond, as recently described [24]. For **II**, **III**, **VII** and **X** the mass increase was obscured by decomposition of ligands, followed by exotherms (not included in table 4). Compounds containing perchlorate were not studied for safety reasons.

For **IV**, **V** and **IX**, their influence on graphite oxidation was studied. From DTG-curves (figure 2) and from characteristic temperatures in TG (table 5) it is apparent

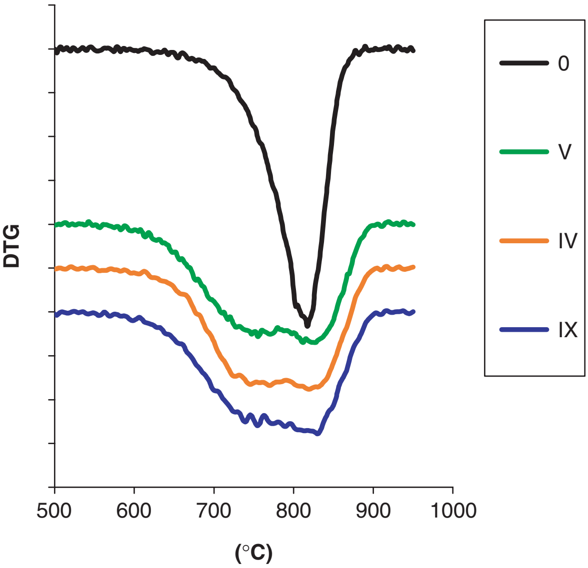

Figure 2. DTG curves of graphite samples containing complexes **IV**, **V** and **IX**. Trace **0** is for pure graphite.

Table 5. Characteristic temperatures (°C) and kinetic parameters of graphite oxidation of selected samples.[a]

Sample		T_p	T_m	T_k	$T_k - T_p$
0		763	818	844	81
V		677	811	867	190
IV		682	819	867	185
IX		675	830	869	194
	Step	n	A (s^{-1})	E (kJ mol^{-1})	w (%)
0		0.8	$2.99 \cdot 10^{10}$	259	
V	I	1.4	$1.01 \cdot 10^{8}$	211	43.9
	II	0.9	$1.79 \cdot 10^{8}$	221	56.1
IV	I	1.5	$5.04 \cdot 10^{8}$	230	50.3
	II	1.0	$9.22 \cdot 10^{9}$	260	49.7
IX	I	1.5	$1.39 \cdot 10^{7}$	200	49.2
	II	0.9	$3.70 \cdot 10^{8}$	228	50.8

[a] T_p = start of oxidation, T_m = oxidation speed maximum, T_k = end of oxidation, n = reaction order, A = frequency factor, E = activation energy, w = mass of sample oxidized.

that the presence of small amounts (0.01%) of the Ni(II) complexes exerts a significant influence on graphite oxidation. Complexes **IV**, **V** and **IX** cause a significant decrease (80–90°C) in the temperature at which oxidation commences, in comparison to pure graphite (curve **0** in figure 2). Oxidation proceeds in two continual steps. In the first, the maximum rate of reaction speed is at about 750°C. In the second, the maximum rate in the presence of complex corresponds to that of pure graphite (see T_m values), but T_k values are a little higher than for pure graphite and the oxidation process is characterized by a larger temperature interval ($T_k - T_p$). Kinetic parameters (table 5) were calculated for one-step oxidation (sample **0**, pure graphite) and two-step oxidation (samples with complexes **IV**, **V**, **IX**). The results show that the mechanism of oxidation in the second step is probably similar for all samples ($n = 0.8$–1.0), whereas the reaction order of the first step is significantly higher ($n = 1.4$–1.5) in the presence of complex. In addition, the activation energies of the first step are lower than for the second step. It is concluded that the presence (even of a trace amount) of complex exhibits a remarkable catalytic influence on graphite oxidation.

Supplementary data

Crystallographic data are deposited at the Cambridge Crystallographic Data Centre, No. CCDC 282964. Copies of the data can be obtained free of charge on application to CCDC, 12 Union Road, Cambridge CB2 1EZ, UK; Fax +441223/336033; Email: deposit@ccdc.cam.ac.uk or http://www.ccdc.cam.ac.uk.

Acknowledgements

The authors would like to thank the Ministry of Education Youth and Sports (grant No. MSM 6198959218) for support of this work. We thank also Professor Zdeněk Trávníček for X-ray data measurements and data reduction and Assoc. Professor Zdeněk Šindelář for magnetochemical measurements.

References

[1] C.A. Tsipis, D.P. Kessissoglou, G.E. Manoussakis. *Chim. Chron., New Series*, **11**, 235 (1982).
[2] C.A. Tsipis, D.P. Kessissoglou, G.A. Katsoulos. *Chim. Chron., New Series*, **14**, 195 (1985).
[3] K. Ramalingam, G. Aravamudan. *Inorg. Chim. Acta*, **128**, 231 (1987).
[4] R. Pastorek, J. Kameníček, F. Březina, Z. Šindelář, E. Jehlářová, N. Duffy, T. Glowiak. *Chem. Papers*, **48**, 317 (1994).
[5] R. Pastorek, J. Kameníček, P. Krystýnková, Z. Šindelář. *Acta Univ. Palacki. Olom. Chemica.*, **39**, 63 (2000).
[6] S. Thirumaran, K. Ramalingam. *Transition Met. Chem.*, **25**, 60 (2000).
[7] *Gmelins Handbuch der Anorganischen Chemie, Nickel*, p. 995, Teil C, Lief. 2, Verlag Chemie, Weinheim (1969).
[8] *Gmelins Handbuch der Anorganischen Chemie, Nickel*, p. 1043, Teil C, Lief. 2, Verlag Chemie, Weinheim (1969).
[9] R. Přibil. *Komplexometrické Titrace*, p. 22, SNTL, Praha (1955).
[10] M. Jureček. *Organická Analýza II*, p. 140, ČSAV, Praha (1957).
[11] V. Slovák. *Thermochim. Acta*, **372**, 175 (2001).
[12] G.M. Sheldrick. *Acta Crystallogr.*, **A46**, 467 (1990).
[13] G.M. Sheldrick. *SHELXL-97, Program for Crystal Structure Refinement*, University of Göttingen, Germany (1997).
[14] M. Nardelli. *J. Appl. Cryst.*, **28**, 659 (1995).
[15] W.J. Geary. *Coord. Chem. Rev.*, **7**, 81 (1971).
[16] R.P. Scholer, E.A. Merbach. *Inorg. Chim. Acta*, **15**, 15 (1975).
[17] L. Ballester, A. Guttierez, M.F. Perpinan, Ruiz-Valero. *Polyhedron*, **15**, 1103 (1996).
[18] I.E. Černikova, I.A. Chartonik, D.S. Umrejko, A.B. Kavrikov, V.I. Afanov. *Koord. Chim.*, **15**, 1695 (1989).
[19] S.V. Larionov, L.A. Patrina, I.M. Oglezneva, E.M. Uskov. *Koord. Chim.*, **10**, 92 (1984).
[20] A.B.P. Lever. *Inorganic Electronic Spectroscopy*, p. 534, Elsevier, Amsterdam (1984).
[21] C.A. Tsipis, D.P. Kessissoglou, G.E. Manoussakis. *Inorg. Chim. Acta*, **65**, L137 (1982).
[22] C.A. Tsipis, I.E. Meleziadis, D.P. Kessissoglou, G.A. Katsoulos. *Inorg. Chim. Acta*, **90**, L19 (1984).
[23] D.R. Lide (Ed.). *Handbook of Chemistry and Physics*, 73rd Edn, CRC Press, Boca Raton (1992).
[24] F. Březina, E. Benátská. *J. Thermal Anal.*, **22**, 75 (1981).